



Analysis of natural organic matter chemistry in bentonite clay under compaction using different dry densities and duration

Meiling Man^a, Huan Tong^a, Nivetha Srikanthan^a, Muhammed O. Usman^a, Claire S. Tully^b, James J. Noël^b, Mehran Behazin^c, W. Jeffrey Binns^c, Peter G. Keech^c, Myrna J. Simpson^{a,*}

^a Environmental NMR Centre and Department of Physical and Environmental Sciences, University of Toronto Scarborough, Toronto, Ontario M1C1A4, Canada

^b Department of Chemistry, Western University, London, Ontario N6A 3K7, Canada

^c Nuclear Waste Management Organization, 22 St. Clair Avenue East, Toronto, Ontario, M4T 2S3, Canada

ARTICLE INFO

Editorial handling by: Daniel S. Alessi

Keywords:

Used nuclear fuel
Deep geological repository
Pressure cell compaction
Extractable lipids
Solid-state ¹³C NMR

ABSTRACT

The Nuclear Waste Management Organization of Canada has adopted an adaptive phased management plan for the long-term storage of used nuclear fuel in a Deep Geological Repository (DGR). The DGR barrier system employs copper-coated used fuel containers (UFCs) surrounded by buffer material which is composed of highly compacted bentonite clay. The natural organic matter (NOM) composition of the compacted bentonite is of practical importance for the safety assessment as it regulates the biogeochemical processes at the interface between the UFCs and the buffer layer. However, insufficient investigations on NOM constituents limits the understanding of biogeochemical dynamics in bentonites compacted under different dry densities. This study analyzed the carbon content and NOM composition using targeted compound analysis and solid-state ¹³C nuclear magnetic resonance (NMR) spectroscopy with bentonites compacted at 1.1, 1.4 or 1.6 g/cm³ dry density for 1, 3, 6, 12 or 18 months. Organic carbon contents were similar across bentonites with different compaction densities at various durations as compared to the reference clay (powdered bentonite sample before compaction). The overall NOM composition measured by solid-state ¹³C NMR suggested a predominance of alkyl and aromatic carbon in bentonite samples. No marked variations were observed for the NOM components (i.e., alkyl, O-alkyl and aromatic carbon) between the compacted bentonites and the reference clay. Targeted compound analysis revealed that the extractable lipid concentrations in the compacted clays did not significantly vary from the reference bentonite with only some compounds exhibiting nano-gram level differences. Bentonites with relatively lower dry densities (1.1 and 1.4 g/cm³) demonstrated slightly higher extractable compound concentrations, but these differences were not statistically significant. In contrast, the compound concentrations of bentonites compacted to 1.6 g/cm³ were similar or slightly lower compared with the reference bentonite, likely associated with limited microbial growth under high dry compaction density. Taken together, these results suggested that NOM composition and quantity did not significantly alter in bentonites under various pressures nor with longer experimental durations. These findings highlight that compacted bentonite exhibited geochemical stability under the simulated repository environments, which provides critical insight for design and performance of engineered barrier system in a DGR concept.

1. Introduction

A long-term solution for the disposal of used nuclear fuel has been investigated by several agencies around the world such as Finland, Switzerland, Canada and the United States (Hall et al., 2021). The

Nuclear Waste Management Organization of Canada is implementing an adaptive phased management plan to isolate and contain used nuclear fuel deep underground utilizing a multibarrier system at a depth of approximately 500–800 m, depending on the host rock (Villagran et al., 2011). The Deep Geological Repository (DGR) will be situated in a

* Corresponding author. Department of Physical and Environmental Sciences and Environmental NMR Centre, University of Toronto Scarborough, 1265 Military Trail, Toronto, ON M1C 1A4, Canada.

E-mail addresses: meiling.man@utoronto.ca (M. Man), phoebe.tong@mail.utoronto.ca (H. Tong), n.srikanthan@utoronto.ca (N. Srikanthan), muhammed.usman@utoronto.ca (M.O. Usman), ctully3@uwo.ca (C.S. Tully), jjnoel@uwo.ca (J.J. Noël), mbehazin@nwmco.ca (M. Behazin), jbinns@nwmco.ca (W.J. Binns), pkeech@nwmco.ca (P.G. Keech), myrna.simpson@utoronto.ca (M.J. Simpson).

<https://doi.org/10.1016/j.apgeochem.2024.105985>

Received 10 October 2023; Received in revised form 22 March 2024; Accepted 25 March 2024

Available online 27 March 2024

0883-2927/© 2024 The Authors. Published by Elsevier Ltd. This is an open access article under the CC BY-NC license (<http://creativecommons.org/licenses/by-nc/4.0/>).

suitable sedimentary or crystalline rock environment and will employ copper-coated used fuel containers (UFCs) surrounded by buffer clay materials (Binns et al., 2023). The buffer clay layer provides sealing protection of the UFCs including minimizing the interaction with groundwater, air and microbial activity near the metal containers and retarding the movement of radionuclides under a container failure scenario. The most ideal candidate for the buffer materials is highly compacted bentonite as it presents desirable inherent properties such as high cation exchange capacity (Bors et al., 1999), high swelling capacity (Wilson and Luczkovich, 2011; Slater et al., 2013), low water activity and low permeability (Stroes-Gascoyne et al., 2010). A variety of Wyoming MX-80 bentonites have been previously investigated to further understand its biophysical and chemical properties, as well as its suitability for being used in the barrier system (Villagran et al., 2011; Wilson and Luczkovich, 2011; Marshall et al., 2015; Usman and Simpson, 2021). These studies observed that organic carbon content in the MX-80 bentonite clay is overall very low within the range of 0.095%–0.28% (Fernandes et al., 2011; Marshall et al., 2015; Usman and Simpson, 2021; Burzan et al., 2022; Tong et al., 2023). The natural organic matter (NOM) in MX-80 bentonite is diagenetically altered, and mostly comprised of aliphatic and aromatic components with low variability amongst different mined batches (Marshall et al., 2015; Usman and Simpson, 2021; Tong et al., 2023). Chemical analyses targeting specific groups of aliphatic lipids revealed that plant-derived long-chain lipids exhibited higher concentrations compared to the short-chain lipids which are primarily derived from microbes (Marshall et al., 2015; Usman and Simpson, 2021; Tong et al., 2023). Moreover, molecular-level analysis observed that bentonite clay NOM compounds were insensitive in response to higher temperature and radiation, and the overall NOM chemistry was unaltered under these treatments (Tong et al., 2023). Even at these low concentrations, the presence of NOM in bentonite can potentially serve as substrates for microbes and promote microbial-induced corrosion of the metal canisters (Stroes-Gascoyne and Hamon, 2008; Stroes-Gascoyne et al., 2011), and thus is a crucial design consideration for the engineered barrier system (EBS). Particularly, the anaerobic microbial processes caused by sulfate-reducing bacteria can utilize a wide range of carbon sources and produce copper-corrosive hydrogen sulfide, thus threatening the integrity of the UFCs (Stroes-Gascoyne and Hamon, 2008; Masurat et al., 2010; Stroes-Gascoyne et al., 2011).

In the EBS design, the powdered bentonite is compacted to >1.70 g/cm³ dry density (high swelling pressures) to form a buffer block, surrounded by gapfill materials which are also composed of the same type of bentonite (Jalique et al., 2016; Binns et al., 2023). The compaction process may alter the microstructure of the montmorillonite in bentonite by reducing the inter-aggregate porosity and disrupting the micro-aggregates (Delage et al., 2006; Likos and Wayllace, 2010). As NOM is mainly preserved via adsorption to mineral surfaces and encapsulation within aggregates which limits bioavailability (Sollins et al., 1996; Mayer et al., 2004), the alteration of the microstructure of bentonite may alter the availability and reactivity of NOM that was protected within the bentonite matrix. A previous investigation observed that during the repetitive compaction process, the soluble NOM concentration increased compared to the un-compacted bentonite, likely associated with the desorption of NOM due to disrupted clay structure (Maanoja et al., 2021). This change may also potentially alter microbial assemblages and activity because the altered NOM in the bentonite buffer can change the substrate source for microbes (Hallbeck, 2010; Villagran et al., 2011; Marshall et al., 2015). Several studies reported that the relatively lower dry density compaction such as 1.3–1.4 g/cm³ (Maanoja et al., 2020) or 1.1–1.5 g/cm³ (Engel et al., 2019) did not fully inhibit microbial growth. However, the compaction of bentonite clay (Wyoming MX-80) up to a dry density of 1.6 g/cm³ was found to suppress bacterial growth and the germination of spores likely associated with limited pore space, low water activity and high swelling pressure (Motamedi et al., 1996; Stroes-Gascoyne et al., 2010; Jalique et al.,

2016). These findings in tandem suggested that the biogeochemical dynamics in bentonite compacted at different dry densities may be altered to various extents, which may pose risks on the integrity and functionality of the UFCs. Properly assessing the potential of bentonite NOM in regulating the biogeochemical processes in the DGR buffer system requires knowledge on the alterations in NOM constituents under specific repository conditions. However, the current understanding regarding the changes in NOM components under different dry density compactions is lacking due to insufficient characterization of NOM in the compacted bentonites. As such, specific investigations on the NOM compositional change are warranted to better understand and predict the biogeochemistry at the interface between the bentonite buffer and UFCs.

This study reports on the NOM composition in bentonite clay that was compacted at different pressures for a range of durations. In this pressure cell experiment, bentonite clay (powdered and gapfill) was compacted to different dry densities of 1.1, 1.4 or 1.6 g/cm³ for durations including 1, 3, 6, 12 or 18 months. Culturing- and DNA-based microbial analyses on these samples observed increased aerobic heterotroph abundances as well as changes in microbial community structure in clays compacted at 1.1 and 1.4 g/cm³ dry densities (Beaver et al., 2024). The shifts in microbial community composition and abundances under various pressure compactions may alter NOM decomposition and constituents. Furthermore, the changes in bentonite clay microstructure during compaction process may either promote the desorption of NOM compounds within the mineral matrix or limit the release of NOM due to the decreasing pore size (Delage et al., 2006; Likos and Wayllace, 2010; Maanoja et al., 2021). As such, it is hypothesized that NOM compound concentrations may vary over time with bentonite compacted to different dry densities relative to the reference clay (powdered bentonite before compaction), and this results in a shift in the overall NOM composition. To test this hypothesis, the compacted samples in tandem with a non-compacted reference bentonite were characterized for its NOM compositional change using both non-targeted (Nuclear Magnetic Resonance, NMR) and targeted compound analytical approaches. The analyses were conducted based on the solid-phase NOM to obtain a holistic view of NOM compositional change, but not on the soluble fraction of NOM. Solid-state ¹³C NMR spectroscopy analysis provides an overview of the NOM composition, while chemical compound analysis using gas chromatography-mass spectrometry (GC-MS) allows a detailed characterization on the extractable aliphatic lipids.

2. Materials and methods

2.1. Pressure cell experiments

A series of pressure vessels were filled with MX-80 bentonite clay, supplied by the Nuclear Waste Management Organization and compacted to different dry densities. The powdered bentonite clay was compacted to 1.1, 1.4, or 1.6 g/cm³. Gapfill bentonite, a granulated bentonite material used to backfill the voids in between the compacted bentonite blocks and the host rock, was compacted to 1.6 g/cm³. The clay plugs are 5.3 cm in diameter and 14.8 cm in height (Tully et al., 2023). The pressure vessel casings were fabricated from 316 stainless steel, with detachable stainless-steel filter stones and end caps. Each pressure vessel was lined with a poly-tetrafluoroethylene (PTFE) inner casing. All pressure vessels were sterilized with 99.5 vol% acetone then to 70 vol% ethanol (Beaver et al., 2024; Tully et al., 2023). Pressure vessel experiments were assembled and disassembled in an oxic environment using a hydraulic press and sterilized bentonite sampling tools, but the oxic condition was not maintained during the incubation (Tully et al., 2023). To accelerate the saturation of the bentonite clay with water during the experiments, vessels were connected to an AZURA P6.1L HPLC pump and pressurized to 10 MPa with naturally aerated Type 1 water, which is purified by a ThermoScientific water system with

resistivity of 18.2 MΩ cm and total oxidizable carbon level <5 ppb. All experiments were conducted at room temperature (21 ± 2°C; Beaver et al., 2024; Tully et al., 2023).

The incubation experiment design includes two replicates for each treatment. Pressure vessels were incubated for 1, 3 and 6 months with the 1.1, 1.4, or 1.6 g/cm³ powdered bentonite, as well as 1, 6 and 18 months for the 1.6 g/cm³ gapfill bentonite. In addition, duplicate pressure vessels for the 1.4 and 1.6 g/cm³ powdered bentonite were also incubated for 18 months. After each incubation, pressure vessels were disassembled, and bentonite clay were isolated and frozen (Beaver et al., 2024; Tully et al., 2023). Because of the trace amount of NOM in MX-80 and sample mass requirements for analysis, bentonite samples from the two replicate pressure cells were combined to form a composite sample. The list of samples analyzed for each dry density, duration and powdered or gapfill bentonite is listed in Table 1. Powdered MX-80 bentonite before compaction was also analyzed as a reference sample. Frozen composite samples were freeze-dried prior to analysis.

2.2. Measurement of total carbon, organic carbon, and inorganic carbon contents

Total carbon, organic carbon and inorganic carbon was determined by the University of Guelph, Laboratory Services. Approximately 2 g of freeze-dried and ground bentonite samples were submitted for analyses. A LECO CN828 carbon analyzer is used to measure total carbon and inorganic carbon; organic carbon is determined by difference. The detection limit for total carbon and inorganic carbon analysis is 0.015%.

2.3. Solid-state ¹³C nuclear magnetic resonance (NMR) spectroscopy

Approximately 80 g of each composite sample was pre-treated to concentrate the organic carbon to be detected using ¹³C NMR spectroscopy. Samples were repeatedly extracted with a mixture of hydrofluoric acid (10%) and hydrochloric acid (4%) with consistent number of treatments (~20 times) for all the samples. After extraction, the samples were then repeatedly rinsed with deionized water to remove residual salts and then freeze-dried. Each extracted sample was then analyzed using solid-state ¹³C NMR spectroscopy. Samples were placed in zirconium 4 mm rotors and sealed with a Kel-F cap. Spectra were acquired with a Bruker Avance III 500 MHz NMR spectrometer (Bruker BioSpin, Rheinstetten, Germany) and a 4 mm H-X MAS probe. A ramp-cross polarization pulse program (Conte et al., 2004), a magic angle spinning rate of 11 kHz, a cross polarization contact time of 1 ms and 1 s recycle delay were used. The NMR analysis was not replicated on each sample

Table 1

Total carbon, inorganic carbon, and organic carbon in bentonite samples used in pressure cell experiments. Sample descriptions are based on the dry density (1.1, 1.4 and 1.6 g/cm³), experimental duration (1, 3, 6, 12 or 18 months), and type (powdered (P) or gapfill (G)). The reference sample was analyzed for carbon contents before compaction.

Sample description	Total carbon (%)	Inorganic carbon (%)	Organic carbon (%)
Reference	0.639	0.551	0.142
1.1-1-P	0.743	0.559	0.163
1.1-3-P	0.757	0.578	0.179
1.1-6-P	0.803	0.576	0.228
1.4-1-P	0.719	0.556	0.163
1.4-3-P	0.825	0.554	0.271
1.4-6-P	0.784	0.633	0.151
1.4-12-P	0.774	0.608	0.166
1.6-1-P	0.669	0.574	0.095
1.6-3-P	0.799	0.587	0.212
1.6-6-P	0.683	0.579	0.104
1.6-12-P	0.736	0.543	0.193
1.6-1-G	0.827	0.686	0.141
1.6-6-G	0.798	0.604	0.195
1.6-18-G	0.850	0.731	0.119

because the analysis result represents an average of thousands of scans and this technique is highly reproducible with measurement errors <1% (Dria et al., 2002; Sun et al., 2019). NMR spectra were processed using Bruker TopSpin (version 3.6) using a line broadening of 100 Hz and calibrated against glycine. The ¹³C NMR spectra were integrated into four general regions: alkyl (0–50 ppm), O-alkyl (50–110 ppm), aromatic and phenolic (110–165 ppm), and carboxyl and carbonyl (165–220 ppm) carbon (Fig. 1) and these regions were normalized to 100% of the total signal.

2.4. Solvent extractable organic matter compounds

Solvent extractable compounds were isolated and analyzed using GC-MS. Approximately 20 g of each bentonite sample was sequentially extracted with 30 mL dichloromethane, dichloromethane:methanol (1:1 v/v) mixture, and methanol for 30 min each using sonication. The extracts were then combined and filtered through glass microfiber filters (Whatman GF/A and GF/F). Filtered extracts were concentrated by rotary evaporation and then dried under a stream of nitrogen gas. Prior to GC-MS analysis, extracts were derivatized with *N,O*-bis-(trimethylsilyl) trifluoroacetamide (BSTFA) and pyridine at 70 °C for 2 h. Derivatized extracts were transferred into a 250 μL vial insert with hexane and then placed inside a 2 mL chromatography vial for analysis. Analysis was carried out with an Agilent 7890B gas chromatograph coupled to a 5977A mass spectrometer equipped with electron impact (70 eV) ionisation. Samples (1 μL) were injected using splitless mode with an inlet temperature of 280 °C onto a HP-5MS fused silica capillary column (30 m length x 0.25 mm diameter x 0.25 μm film thickness). A gradient oven temperature program was used as follows: 65 °C was held for 2 min followed by a 6 °C/min ramping until 300 °C and then held for 20 min. Helium was used as a carrier gas at a flow rate of 1 mL/min. Data acquisition was performed using Agilent Mass Hunter software (version B.March 07, 2129) and data were processed using Agilent Enhanced Chemstation software (version F.March 01, 2357). External standards used for quantification were tetracosane (analytical standard grade, ≥99.5%, Sigma-Aldrich), methyl tricosanoate (analytical standard

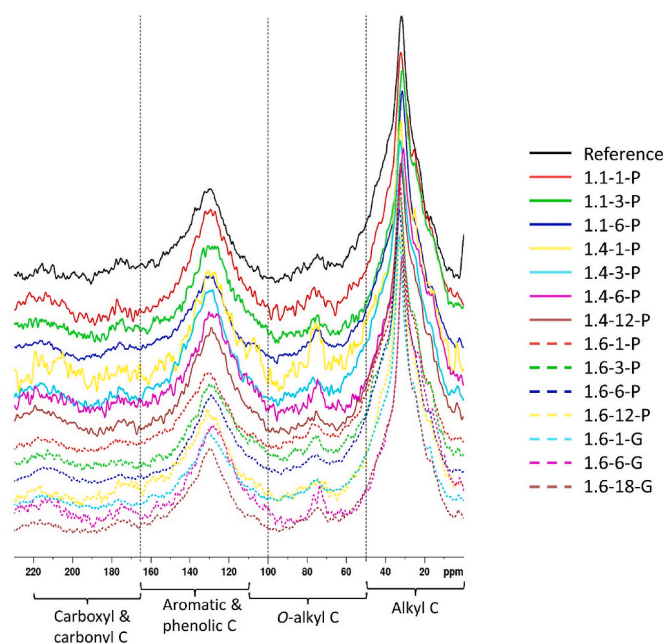


Fig. 1. Solid-state ¹³C Nuclear Magnetic Resonance (NMR) spectra of the reference sample and compacted bentonites with different dry densities (1.1, 1.4 or 1.6 g/cm³), experimental durations (1, 3, 6, 12 or 18 months), and types (powdered (P) or gapfill (G)). The NMR analysis on the reference sample was conducted before compaction.

grade, $\geq 99.0\%$, Sigma-Aldrich), 1-docosanol (Approximately 98%, Sigma-Aldrich) and cholesterol (analytical standard grade, $\geq 99.0\%$, Sigma-Aldrich). The GC-MS analysis is highly sensitive with instrumental limits of detection ranging from 12 to 100 pg (Usman and Simpson, 2021). Details of instrumental detection and quantification limits are provided in Usman and Simpson (2021). Compound concentrations were corrected against method blanks. Compounds were identified using Wiley Registry (9th edition) plus NIST (2014 version) mass spectral databases, and published mass spectra. Each bentonite sample was extracted in triplicate.

2.5. Statistical analyses

Analysis of variance (ANOVA) was performed using IBM SPSS (version 22) to examine statistically significant differences with treatments. One-way ANOVA followed by Tukey's post hoc test assessed significant differences ($P < 0.05$) in targeted compound concentrations between the reference sample and treated bentonite samples. The targeted compound concentrations were compared as: individual compound concentrations; the sum of short-chain ($< C_{20}$) and long-chain ($\geq C_{20}$) *n*-alkanes, *n*-alkanols and *n*-alkanoic acid concentrations; total concentration of all *n*-alkanes, total concentration of all *n*-alkanols and total concentration of all *n*-alkanoic acids; and total concentration of all solvent extractable compounds. Principal component analysis (PCA) was performed to illustrate the variations across different compacted bentonites based on the concentrations of short-chain, long-chain *n*-alkanes, *n*-alkanols and *n*-alkanoic acids. A heatmap was created to better demonstrate the relative percentage changes of compacted bentonites compared to the reference for the individual extractable compounds. PCA and heatmap analysis were conducted using R (version 4.1.2).

3. Results and discussion

3.1. Carbon content analysis

The total carbon content of all the samples ranged between 0.64% and 0.85% with an average of 0.76% (Table 1). The lowest carbon content was observed with the reference bentonite while the highest value was found with a gapfill sample at 1.6 g/cm³ dry density after 18 months of incubation (1.6–18-G). The inorganic carbon content is between 0.54% and 0.73% across all bentonite clays and contributes a major fraction to the total carbon (Table 1). The organic carbon only accounts for a small portion (14%–33%) of the total carbon, and varies within the range of 0.095%–0.27% across the reference and samples with various dry densities (Table 1). The highest organic carbon content was observed in the sample with 1.4 g/cm³ dry density compaction (1.4-3-P), while the lowest concentration was found with a high dry density sample (1.6-1-P). Previous investigations on other MX-80 bentonite clays (without treatments) reported organic carbon content ranging from 0.095% to 0.28% (Fernandes et al., 2011; Marshall et al., 2015; Usman and Simpson, 2021; Burzan et al., 2022; Tong et al., 2023). The comparison of the organic carbon range in this study with the previous reported values suggests that organic carbon contents with different dry densities are within the previously reported variability range (Marshall et al., 2015; Usman and Simpson, 2021). Therefore, these results suggest that the variation in organic carbon content under different dry density compaction and durations were very low and that they did not exceed the threshold of the natural heterogeneity of bentonite previously quantified (Usman and Simpson, 2021).

3.2. Solid-state ¹³C nuclear magnetic resonance (NMR) analysis of natural organic matter (NOM) in compacted bentonites

Solid-state ¹³C NMR spectroscopic analysis reveals the overall compositional characteristics of the NOM in bentonite clays. The area integration based on specific chemical shift ranges indicates the relative

percentage of particular types of NOM constituents (Baldock et al., 1992). The predominant components in the reference and compacted MX-80 clay NOM are the alkyl carbon which is mainly derived from cutin, suberin and aliphatic lipids, as well as aromatic carbon which primarily comes from black carbon and lignin (Baldock et al., 1992, Table 2). These two constituents account for approximately 78%–85% of the total carbon (Table 2). These results are consistent with another study on the NOM compositional variability in different sourced MX-80 bentonites, which reported that the alkyl and aromatic carbon typically contribute up to 80% to the overall carbon pool (Usman and Simpson, 2021). In general, the alkyl and aromatic carbon content were similar across different dry density bentonites relative to the reference clay (Fig. 2; Table 2). The *O*-alkyl carbon, which is mainly from cellulose and simple sugars (Baldock et al., 1992), varies from 9% to 16% with small differences relative to the reference (within $\pm 4\%$; Table 2). As such, *O*-alkyl carbon did not demonstrate substantial changes across different dry density samples nor with various durations. The carboxyl and carbonyl carbon can be derived from a range of sources such as fatty acids, amino acids and peptides, and did not exhibit marked changes across the compacted bentonite clays (Table 2). As the *O*-alkyl carbon often serves as preferred substrates for microbes compared with alkyl carbon, the ratio of the alkyl over *O*-alkyl carbon is widely used to assess the NOM degradation status with a higher value indicating more enhanced NOM decomposition (Baldock et al., 1992; Simpson and Simpson, 2012). The alkyl/*O*-alkyl carbon varied between 3.4 and 6.2 (Table 2), suggesting a relatively high extent of diagenetic alteration. Overall, when examining the potential controls of different dry density compaction and durations on specific carbon components, no consistent trends were observed with increasing dry density compaction treatments nor with longer durations. A previous study investigated the natural heterogeneity in MX-80 from different deposits and batches and reported that the variabilities for the individual NOM component span between 1% and 5% and that the alkyl/*O*-alkyl carbon ratio ranges between 3.1 and 7.4 (Usman and Simpson, 2021). Therefore, although the NOM diagenetic state exhibited some variability across different samples, these differences were likely related to the inherent natural heterogeneity of the bentonite clays (Usman and Simpson, 2021). These results suggest that the compacted bentonites did not demonstrate marked changes in the NOM composition with different dry densities (Fig. 1). Taken together, the characterization on the NOM composition using solid-state ¹³C NMR suggests that the overall NOM distribution and constituents were not altered with specific dry density compactions

Table 2

Solid-state ¹³C Nuclear Magnetic Resonance (NMR) analysis integral results of the reference sample and compacted bentonites. The NMR analysis on the reference sample was conducted before compaction. Sample descriptions are based on the dry density (1.1, 1.4 and 1.6 g/cm³), experimental duration (1, 3, 6, 12 or 18 months), and type (powdered (P) or gapfill (G)).

Sample Description	Alkyl carbon	<i>O</i> -alkyl carbon	Aromatic & phenolic carbon	Carboxyl & carbonyl carbon	Alkyl/ <i>O</i> -alkyl carbon ratio
Reference	52	12	28	8	4.33
1.1-1-P	51	13	29	7	3.92
1.1-3-P	56	10	27	7	5.60
1.1-6-P	55	12	26	7	4.58
1.4-1-P	51	15	27	7	3.40
1.4-3-P	51	13	30	6	3.92
1.4-6-P	55	9	28	8	6.11
1.4-12-P	56	9	28	7	6.22
1.6-1-P	57	13	26	4	4.38
1.6-3-P	57	15	24	4	3.80
1.6-6-P	56	15	25	4	3.73
1.6-12-P	54	11	28	7	4.91
1.6-1-G	55	16	25	4	3.44
1.6-6-G	54	11	27	8	4.91
1.6-18-G	59	11	26	4	5.36

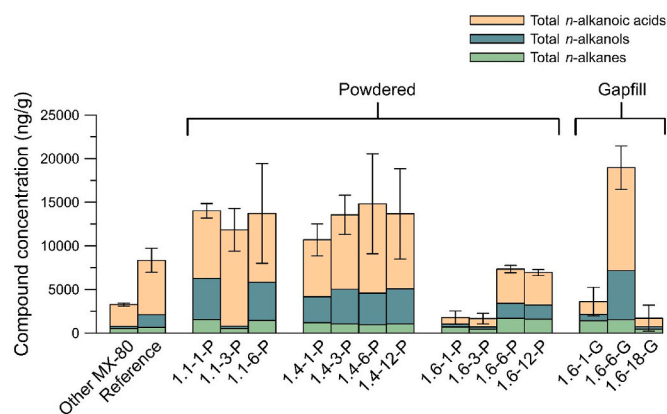


Fig. 2. Concentrations of total *n*-alkanes, *n*-alkanols and *n*-alkanoic acids isolated from bentonite clay samples with different dry densities (1.1, 1.4 or 1.6 g/cm³), experimental durations (1, 3, 6, 12 or 18 months), and types (powdered (P) or gapfill (G)); Error bars indicate the standard errors ($n = 3$) of the mean based on the concentrations of all solvent extractable compounds. No statistically significant ($P < 0.05$) changes were observed for total concentrations of *n*-alkanes, *n*-alkanols, *n*-alkanoic acids and all compounds compared with the reference. Data of other MX-80 are summarized from Usman and Simpson (2021) and Tong et al. (2023). Detailed concentration and compound distribution are listed in Tables S1–S2.

nor durations.

3.3. Natural organic matter (NOM) compositional characteristics revealed by targeted compound analysis

The targeted chemical analysis elucidates the extractable lipids mainly including *n*-alkanes, *n*-alkanols and *n*-alkanoic acids (Otto and Simpson, 2005; Usman and Simpson, 2021; Tong et al., 2023). The total concentrations of these compounds ranged between 1659 (± 604) and 18,956 (± 2498) ng/g clay across the bentonite samples but did not exhibit significant differences when compared to the reference clay. Analyses with the individual compound distribution suggested that the extracted aliphatic lipids of the compacted bentonites exhibited similar concentrations as compared to the reference (Fig. 2 and Tables S1–S2). Some differences were observed at the nanogram level (ng/g clay) with 1.1-1-P (C₂₆ alkanol), 1.1-6-P (C₂₄ alkanol), 1.6-6-G (C₁₄, C₁₈ alkanols; C₈, C₉, C₁₂ alkanolic acids) and 1.6-12-P (C₃₁ alkane; Tables S1–S2). Among the extracted compounds, the short-chain and long-chain lipids are categorized into different groups because they are reported to primarily come from different sources (Bianchi, 1995; Lichtfouse et al., 1995). Long-chain *n*-alkanes, *n*-alkanoic acids and *n*-alkanols are mainly vascular plant-derived (Bianchi, 1995), while short-chain aliphatic lipids are likely from different origins. For instance, short-chain (<C₂₀) *n*-alkanes can be attributed from both plant and microbial sources and short-chain *n*-alkanoic acids typically originate from a variety of sources such as plant, microbes as well as moss and thus are less source-indicative (Bianchi, 1995; Volkman et al., 2008). Short-chain *n*-alkanols are predominantly derived from microbes (Volkman et al., 2008). Compared with the reference sample, short-chain and long-chain *n*-alkane and *n*-alkanoic acid concentrations did not significantly differ across various compacted bentonites. Short-chain and long-chain *n*-alkanols were also consistent across compacted bentonites except for short-chain *n*-alkanols under a 1.6 g/cm³ dry density gapfill sample (1.6-6-G) where they were relatively higher (Fig. 3). However, the samples under the same compaction treatment (1.6 g/cm³ gapfill) but at different durations (1 or 18 months) demonstrate overall consistency or slightly decreased concentrations relative to the reference for short-chain *n*-alkanols.

Noticeably, long-chain *n*-alkanes contain approximately 4–21 times the abundance than their short-chain counterpart (Fig. 4). In contrast,

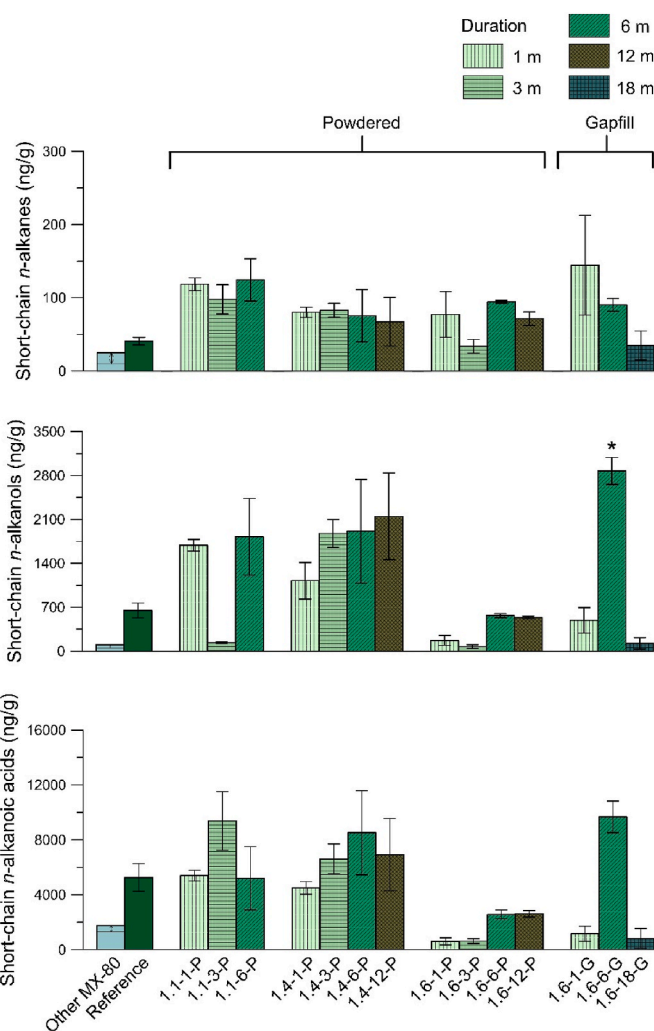


Fig. 3. Concentrations of short-chain *n*-alkanes, *n*-alkanols and *n*-alkanoic acids isolated from bentonite clay samples with different dry densities (1.1, 1.4 or 1.6 g/cm³), experimental durations (1, 3, 6, 12 or 18 months), and types (powdered (P) or gapfill (G)); significant differences ($P < 0.05$) compared to the reference sample are marked with an asterisk. Data of other MX-80 are summarized from Usman and Simpson (2021) and Tong et al. (2023), with the arrows indicating the variability range of concentrations from MX-80 bentonites. Detailed concentration and compound distribution are listed in Tables S1–S2.

short-chain *n*-alkanoic acids exhibited an overall (2–13 times) higher concentration than the long-chain *n*-alkanoic acids. However, the higher content for the short-chain *n*-alkanoic acids is likely associated with the presence of C₁₆ and C₁₈ analogues which can be found ubiquitously among an array of sources such as plants, animals, diatom, algae and bacteria (Bianchi, 1995; Volkman et al., 2008; Bechtel and Schubert, 2009; Mortillaro et al., 2011). The content of C₁₆ and C₁₈ *n*-alkanoic acids are often excluded in the calculation of short-chain *n*-alkanoic lipids (Usman and Simpson, 2021; Tong et al., 2023). In the present study, the concentration of short-chain *n*-alkanoic acids without the C₁₆ and C₁₈ analogues was overall lower compared to their long-chain counterparts for most bentonite samples. These results also agreed with previous findings on MX-80 that observed lower concentration of short-chain than long-chain *n*-alkanoic acids after the exclusion of C₁₆ and C₁₈ acids (Usman and Simpson, 2021; Tong et al., 2023). Taken together, long-chain aliphatic lipids demonstrated a higher contribution than short-chain lipids to the total extractable compounds. This corroborates that vascular plant materials are the predominant source for the bentonite NOM while microbial contributions are less prevalent

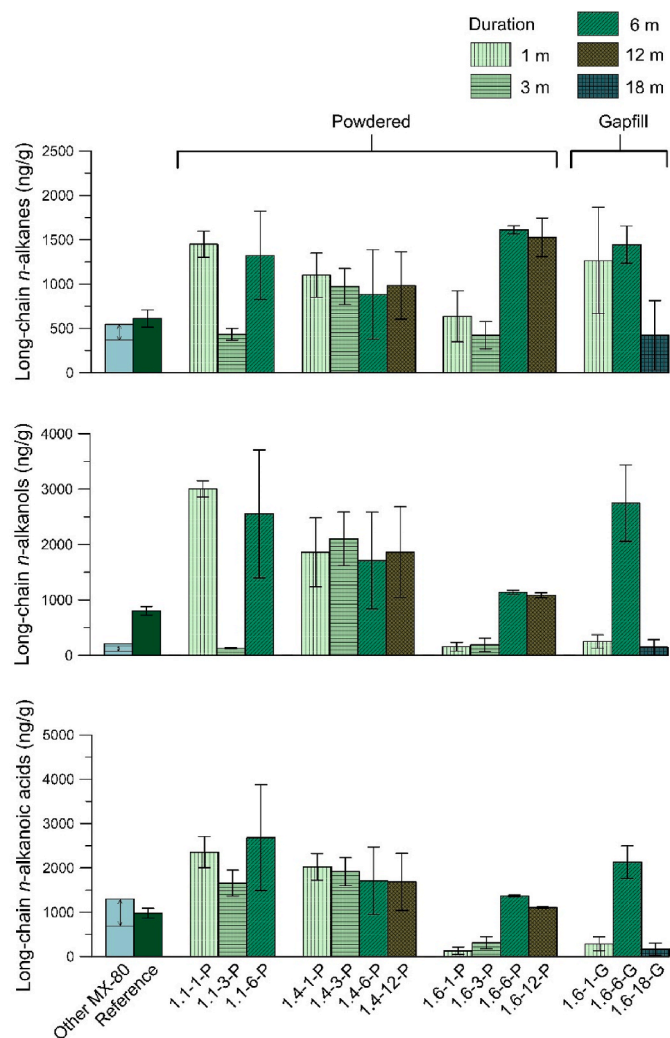


Fig. 4. Concentrations of long-chain *n*-alkanes, *n*-alkanols and *n*-alkanoic acids isolated from bentonite clay samples with different dry densities (1.1, 1.4 or 1.6 g/cm³), experimental durations (1, 3, 6, 12 or 18 months), and types (powdered (P) or gapfill (G)); no significant differences ($P < 0.05$) compared to the reference sample were observed. Data of other MX-80 are summarized from Usman and Simpson (2021) and Tong et al. (2023), with the arrows indicating the variability range of concentrations from MX-80 bentonites. Detailed concentration and compound distribution are listed in Tables S1–S2.

(Marshall et al., 2015; Usman and Simpson, 2021; Tong et al., 2023). Moreover, these NOM components were predominantly preserved in the compacted bentonites and did not exhibit significant differences at the molecular-level compared with the reference bentonite.

3.4. Extractability of natural organic matter (NOM) compounds in response to various dry density compactions

To obtain an overview of the variations among bentonite samples under different compaction densities and durations, PCA was performed using the concentrations of short-chain and long-chain aliphatic lipid indices. The first two axes explained 89% of the variation across all the samples (Fig. 5). The samples are color-coded and grouped based on either different dry densities (Fig. 5a) or durations (Fig. 5b) to better illustrate the variations as a function of compaction treatments and experiment time. The results showed that the groupings with various dry densities overlapped with each other and further suggested that NOM compound composition was overall similar in bentonites with varied dry densities. Similar results were observed with the groupings based on different durations, indicating that longer experimental periods did not substantially shift NOM composition in the compacted clay.

Under different dry compaction densities, a closer inspection revealed that the concentrations of total extractable compounds were on average slightly higher than the reference for the 1.1 and 1.4 g/cm³ dry density samples but these results were not statistically significant. This pattern was not observed with the highest dry density bentonite as most of the samples with 1.6 g/cm³ compaction demonstrated similar or slightly lower compound concentrations than the reference. Similarly, *n*-alkanoic acid and *n*-alcohol compounds also exhibit slightly increased contents with 1.1 and 1.4 g/cm³ samples and slightly decreased concentrations with the 1.6 g/cm³ compacted bentonites but these variations were not significant. To obtain a better understanding on the distribution of the lipids for different treatments, a heatmap demonstrating the percentage change relative to the reference for each individual compound was plotted (Fig. 6). The blue colored cells indicate negative percentage changes, suggesting a decrease in content relative to the reference clay, and vice versa for the red color. The heatmap showed that most of the decreases were observed with the 1.6 g/cm³ dry density under 1 and 3 months of incubation for powdered bentonite, and 1 and 19 months for gapfill materials (Fig. 6). While the positive percentage change is mainly observed with the 1.1 and 1.4 g/cm³ dry density clays (Fig. 6). Overall, these results suggest that bentonites with relatively lower dry densities demonstrate slightly higher concentrations in the extractable NOM compounds. However, the organic carbon contents as well as the overall NOM composition indicated by the NMR analysis demonstrated that the results were within the natural variability range as previously reported in bentonite clay studies (Marshall et al., 2015; Usman and Simpson, 2021; Tong et al., 2023). As such, the

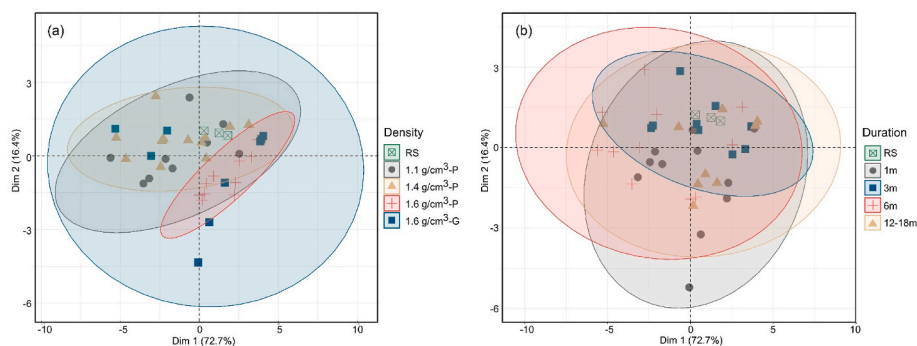


Fig. 5. Principal component analysis based on various NOM indices from reference sample (RS) and bentonites with different dry densities (1.1, 1.4 or 1.6 g/cm³), experimental durations (1, 3, 6, 12 or 18 months), and types (powdered (P) or gapfill (G)). The samples are color-coded and grouped based on specific dry densities (a) and durations (b). A more detailed version of this figure with sample label information is available in Fig. S1.

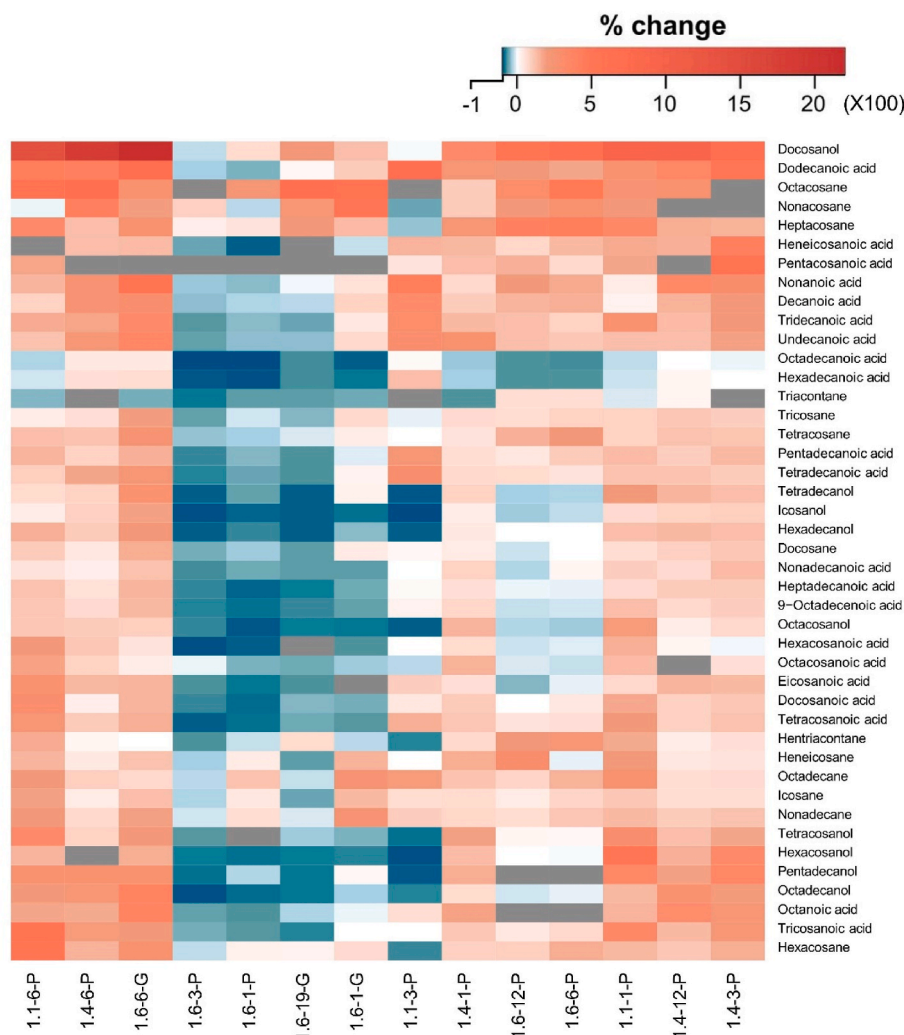


Fig. 6. Heatmap showing percentage changes of compacted bentonites relative to the reference for individual solvent extractable compound. The grey cells indicate no available data. The darker color in red (or blue) indicates a higher positive (or negative) percentage change relative to the reference sample.

slightly higher extracted compound concentrations did not reflect a significant alteration in the stability of NOM in the bentonite clay. It is important to note that several mechanisms have been reported to potentially contribute to the overall changes in bentonite NOM. Previous investigations reported that high pressure compaction process can disrupt the microstructure of the clay minerals (Delage et al., 2006; Likos and Wayllace, 2010) and result in the dissociation of NOM that was previously bound to mineral surfaces or occluded within the microaggregates (Sollins et al., 1996; Angst et al., 2017; Broz, 2020). Moreover, it is reported that relatively lower dry density compaction (i. e., 1.1, 1.4 or 1.5 g/cm³) did not completely restrict microbial growth and activity (Engel et al., 2019; Maanoja et al., 2020), which may result in the degradation of bentonite NOM macromolecules (Kleber et al., 2015; Zhou et al., 2019; Maanoja et al., 2021). Microbial growth and composition were also investigated using culturing- and DNA-based analyses for the compacted bentonites in this study. The results suggested an increase in aerobic heterotroph abundance with the 1.1 and 1.4 g/cm³ compacted samples (Beaver et al., 2024). As such, the disruption of clay mineral and aggregate structure as well as microbial processing can enhance the extractability of NOM compounds under lower dry density compaction (such as 1.1 and 1.4 g/cm³). However, even if these processes were occurring, the potential variations may be too small and were within the natural heterogeneity range, which did not demonstrate statistical significance in our study. Therefore, there was no overall evidence for alterations in NOM composition under the

relatively lower dry density compactations. Interestingly, when the dry density was increased to 1.6 g/cm³, similar contents or slight decreases in the extracted compounds were observed, indicating higher stability in the bentonite NOM. Microbial analysis on the compacted clay samples in this study found that microbial growth was highly suppressed in the 1.6 g/cm³ compacted samples (Beaver et al., 2024). This observation is in agreement with other studies reporting that microbial activities were highly prohibited when bentonite clay was compacted up to a dry density of 1.6 g/cm³ (Motamedi et al., 1996; Stroes-Gascoyne et al., 2010; Jalique et al., 2016). The reduction in microbial decomposition and processing may likely account for the stability of the NOM compounds in clay samples. Although some variations were observed in the lipid concentrations, these differences were not statistically significant suggesting that changes to NOM chemistry due to microbial processes as reported by Beaver et al. (2024) were smaller than the range of natural variability of NOM in MX-80 bentonites. As such, solid-phase NOM in the bentonite clay exhibited geochemical stability under different dry density compaction treatments and durations (1–18 months). Furthermore, similar or lower extractability of solid-phase bentonite NOM in tandem with the consistent findings of prohibited microbial activities (Jalique et al., 2016; Beaver et al., 2024) under 1.6 g/cm³ suggest that bentonite compacted higher than this threshold may exhibit greater stability and is of practical importance for the safety assessment of the DGR.

4. Conclusions

In summary, organic carbon contents for the bentonite clays ranged from 0.095% to 0.27% across different compacted bentonites and the reference clay. The overall NOM composition revealed by solid-state ^{13}C NMR analysis demonstrated a predominance of alkyl and aromatic carbon up to 85% of the total NOM pool. The results of the analyzed NOM constituents such as alkyl, *O*-alkyl and aromatic carbon did not vary beyond the natural variability range of bentonite clay. Targeted compound characterization observed that the concentrations of extractable lipids among the bentonites with different compactions did not significantly vary from the reference bentonite, except for several compounds that exhibited nanogram-level differences. Although bentonites with relatively lower dry densities (1.1 and 1.4 g/cm³) exhibited slightly higher extractable compound abundances, these differences were not statistically significant and is likely related to the natural heterogeneity of the bentonite clays or microbial growth. In contrast, the isolation of solvent extractable NOM components from bentonites compacted to 1.6 g/cm³ was similar or slightly lower relative to the reference, and is consistent with suppressed microbial growth under high density compaction. Overall, bentonite compacted at different dry densities for various durations did not significantly alter the solid-phase NOM quantity and composition, which differs from our original hypothesis that predicted changes in NOM composition under dry density compactions. These findings highlight that the compacted MX-80 bentonite exhibited geochemical stability under the simulated repository conditions. It is also important to note that due to sample size limitations the present study did not involve investigations in dissolved forms of NOM which is more mobile and dynamically reactive, especially with microbial processes. Dissolved NOM may exhibit distinct dynamics compared with the solid-phase NOM, especially under the relatively lower dry density compaction and shorter durations. Further studies on the soluble form of NOM are needed to provide a more holistic view of the biogeochemical dynamics in the bentonite clay, which is a key component for the safety evaluation at the interface between the buffer system and UFCs.

CRediT authorship contribution statement

Meiling Man: Writing – review & editing, Writing – original draft, Validation, Formal analysis. **Huan Tong:** Writing – review & editing, Writing – original draft, Formal analysis, Data curation. **Nivetha Srikanthan:** Writing – review & editing, Validation, Formal analysis, Data curation. **Muhammed O. Usman:** Writing – review & editing, Visualization, Investigation, Data curation. **Claire S. Tully:** Writing – review & editing, Methodology, Conceptualization. **James J. Noël:** Writing – review & editing, Supervision, Methodology, Conceptualization. **Mehran Behazin:** Writing – review & editing, Resources, Project administration, Conceptualization. **W. Jeffrey Binns:** Writing – review & editing, Resources, Project administration, Conceptualization. **Peter G. Keech:** Writing – review & editing, Resources, Project administration, Conceptualization. **Myrna J. Simpson:** Writing – review & editing, Supervision, Resources, Project administration, Funding acquisition.

Declaration of competing interest

The authors declare that they have no known competing financial interests or personal relationships that could have appeared to influence the work reported in this paper.

Data availability

Data will be made available on request.

Acknowledgements

This research was supported by the Natural Sciences and Engineering Research Council (NSERC) of Canada Collaborative Research and Development Grant to M.J.S. and the Nuclear Waste Management Organization, Toronto, Ontario. M.J.S. also thanks NSERC for support via a Tier 1 Canada Research Chair in Integrative Molecular Biogeochemistry. We sincerely thank Dr. Ronald Soong for assistance with NMR acquisition.

Appendix A. Supplementary data

Supplementary data to this article can be found online at <https://doi.org/10.1016/j.apgeochem.2024.105985>.

References

- Angst, G., Mueller, K.E., Kögel-Knabner, I., Freeman, K.H., Mueller, C.W., 2017. Aggregation controls the stability of lignin and lipids in clay-sized particulate and mineral associated organic matter. *Biogeochemistry* 132, 307–324. <https://doi.org/10.1007/s10533-017-0304-2>.
- Baldock, J.A., Oades, J.M., Waters, A.G., Peng, X., Vassallo, A.M., Wilson, M.A., 1992. Aspects of the chemical structure of soil organic materials as revealed by solid-state ^{13}C NMR spectroscopy. *Biogeochemistry* 16, 1–42. <https://doi.org/10.1007/BF00024251>.
- Beaver, R.C., Vachon, M.A., Tully, C.S., Engel, K., Spasov, E., Binns, W.J., Noël, J.J., Neufeld, J.D., 2024. Impact of dry density and incomplete saturation on microbial growth in bentonite clay for nuclear waste storage. *J. Appl. Microbiol.* <https://doi.org/10.1093/jambio/lxae053>.
- Bechtel, A., Schubert, C.J., 2009. A biogeochemical study of sediments from the eutrophic Lake Lugano and the oligotrophic Lake Brienz, Switzerland. *Org. Geochem.* 40, 1100–1114. <https://doi.org/10.1016/j.orggeochem.2009.06.009>.
- Bianchi, G., 1995. Plant waxes. In: Hamilton, R.J. (Ed.), *Waxes: Chemistry, Molecular Biology and Functions*. The Oily Press, Dundee, pp. 175–222.
- Binns, W.J., Behazin, M., Briggs, S., Keech, P.G., 2023. An overview of the Canadian nuclear waste corrosion program. *Mater. Corros.* 2023, 1–7. <https://doi.org/10.1002/maco.202313763>.
- Bors, J., Dultz, St, Riebe, B., 1999. Retention of radionuclides by organophilic bentonite. *Eng. Geol.* 54, 195–206. [https://doi.org/10.1016/S0013-7952\(99\)00074-5](https://doi.org/10.1016/S0013-7952(99)00074-5).
- Broz, A.P., 2020. Organic matter Preservation in ancient soils of earth and mars. *Life* 10, 113. <https://doi.org/10.3390/life10070113>.
- Burzan, N., Murad Lima, R., Fruttschi, M., Janowczyk, A., Reddy, B., Rance, A., Diomidis, N., Bernier-Latmani, R., 2022. Growth and persistence of an aerobic microbial community in Wyoming bentonite MX-80 despite anoxic in situ conditions. *Front. Microbiol.* 13 <https://doi.org/10.3389/fmicb.2022.858324>.
- Conte, P., Spaccini, R., Piccolo, A., 2004. State of the art of CPMAS ^{13}C -NMR spectroscopy applied to natural organic matter. *Prog. Nucl. Magn. Reson. Spectrosc.* 44, 215–223. <https://doi.org/10.1016/j.pnmrs.2004.02.002>.
- Delage, P., Marcial, D., Cui, Y.J., Ruiz, X., 2006. Ageing effects in a compacted bentonite: a microstructure approach. *Geotechnique* 56, 291–304. <https://doi.org/10.1680/geot.2006.56.5.291>.
- Dria, K.J., Sachleben, J.R., Hatcher, P.G., 2002. Solid-state carbon-13 nuclear magnetic resonance of humic acids at high magnetic field strengths. *J. Environ. Qual.* 31, 393–401. <https://doi.org/10.2134/jeq2002.3930>.
- Engel, K., Ford, S.E., Coyotzi, S., McKelvie, J., Diomidis, N., Slater, G., Neufeld, J.D., 2019. Stability of microbial community profiles associated with compacted bentonite from the grimsel underground research laboratory. *mSphere* 4, e00601. <https://doi.org/10.1128/mSphere.00601-19.19>.
- Fernandes, M.F., Barreto, A.C., Mendes, I.C., Dick, R.P., 2011. Short-term response of physical and chemical aspects of soil quality of a kaolinitic Kandiuadals to agricultural practices and its association with microbiological variables. *Agric. Ecosyst. Environ.* 142, 419–427. <https://doi.org/10.1016/j.agee.2011.07.002>.
- Hall, D.S., Behazin, M., Jeffrey Binns, W., Keech, P.G., 2021. An evaluation of corrosion processes affecting copper-coated nuclear waste containers in a deep geological repository. *Prog. Mater. Sci.* 118, 100766 <https://doi.org/10.1016/j.pmatsci.2020.100766>.
- Hallbeck, L., 2010. *Principal Organic Materials in a Repository for Spent Nuclear Fuel* (No. 1404–0344). Sweden.
- Jalique, D.R., Stroes-Gascoyne, S., Hamon, C.J., Priyanto, D.G., Kohle, C., Evenden, W.G., Wolfardt, G.M., Grigoryan, A.A., McKelvie, J., Korber, D.R., 2016. Culturability and diversity of microorganisms recovered from an eight-year old highly-compacted, saturated MX-80 Wyoming bentonite plug. *Appl. Clay Sci.* 126, 245–250. <https://doi.org/10.1016/j.clay.2016.03.022>.
- Kleber, M., Eusterhues, K., Keilueit, M., Mikutta, C., Mikutta, R., Nico, P.S., 2015. Mineral–organic associations: formation, properties, and relevance in soil environments. *Adv. Agron.* 130, 1–140. <https://doi.org/10.1016/BS.AGRON.2014.10.005>.
- Lichtfouse, É., Berthier, G., Houot, S., Barriuso, E., Bergheaud, V., Vallaes, T., 1995. Stable carbon isotope evidence for the microbial origin of C₁₄–C₁₈ n-alkanoic acids in soils. *Org. Geochem.* 23, 849–852. [https://doi.org/10.1016/0146-6380\(95\)80006-D](https://doi.org/10.1016/0146-6380(95)80006-D).

- Likos, W.J., Wayllace, A., 2010. Porosity evolution of free and confined bentonites during interlayer hydration. *Clays Clay Miner.* 58, 399–414. <https://doi.org/10.1346/CCMN.2010.0580310>.
- Maanoja, S., Lakaniemi, A.M., Lehtinen, L., Salminen, L., Auvinen, H., Kokko, M., Palmroth, M., Muuri, E., Rintala, J., 2020. Compacted bentonite as a source of substrates for sulfate-reducing microorganisms in a simulated excavation-damaged zone of a spent nuclear fuel repository. *Appl. Clay Sci.* 196, 105746. <https://doi.org/10.1016/J.CLAY.2020.105746>.
- Maanoja, S., Palmroth, M., Salminen, L., Lehtinen, L., Kokko, M., Lakaniemi, A.M., Auvinen, H., Kiczka, M., Muuri, E., Rintala, J., 2021. The effect of compaction and microbial activity on the quantity and release rate of water-soluble organic matter from bentonites. *Appl. Clay Sci.* 211, 106192. <https://doi.org/10.1016/J.CLAY.2021.106192>.
- Marshall, M.H.M., McKelvie, J.R., Simpson, A.J., Simpson, M.J., 2015. Characterization of natural organic matter in bentonite clays for potential use in deep geological repositories for used nuclear fuel. *Appl. Geochem.* 54, 43–53. <https://doi.org/10.1016/J.APGEOCHEM.2014.12.013>.
- Masurat, P., Eriksson, S., Pedersen, K., 2010. Microbial sulphide production in compacted Wyoming bentonite MX-80 under in situ conditions relevant to a repository for high-level radioactive waste. *Appl. Clay Sci.* 47, 58–64. <https://doi.org/10.1016/j.clay.2009.01.004>.
- Mayer, L.M., Schick, L.L., Hardy, K.R., Wagai, R., McCarthy, J., 2004. Organic matter in small mesopores in sediments and soils. *Geochim. Cosmochim. Acta* 68, 3863–3872. <https://doi.org/10.1016/j.gca.2004.03.019>.
- Mortillaro, J.M., Abril, G., Moreira-Turcq, P., Sobrinho, R.L., Perez, M., Meziane, T., 2011. Fatty acid and stable isotope ($\delta^{13}\text{C}$, $\delta^{15}\text{N}$) signatures of particulate organic matter in the lower Amazon River: seasonal contrasts and connectivity between floodplain lakes and the mainstem. *Org. Geochem.* 42, 1159–1168. <https://doi.org/10.1016/j.orggeochem.2011.08.011>.
- Motamedi, M., Karland, O., Pedersen, K., 1996. Survival of sulfate reducing bacteria at different water activities in compacted bentonite. *FEMS Microbiol. Lett.* 141, 83–87. <https://doi.org/10.1111/j.1574-6968.1996.tb08367.x>.
- Otto, A., Simpson, M.J., 2005. Degradation and preservation of vascular plant-derived biomarkers in grassland and forest soils from western Canada. *Biogeochemistry* 74, 377–409. <https://doi.org/10.1007/s10533-004-5834-8>.
- Simpson, M.J., Simpson, A.J., 2012. The chemical ecology of soil organic matter molecular constituents. *J. Chem. Ecol.* 38, 768–784. <https://doi.org/10.1007/s10886-012-0122-x>.
- Slater, G.F., Moser, D.P.M., Sherwood Lollar, B., 2013. *Development of Microbial Characterization Techniques for Low-Permeability Sedimentary Rocks*.
- Sollins, P., Homann, P., Caldwell, B.A., 1996. Stabilization and destabilization of soil organic matter: mechanisms and controls. *Geoderma* 74, 65–105. [https://doi.org/10.1016/S0016-7061\(96\)00036-5](https://doi.org/10.1016/S0016-7061(96)00036-5).
- Stroes-Gascoyne, S., Hamon, C.J., 2008. The Effect of Intermediate Dry Densities ($1.1\text{--}1.5\text{ G/cm}^3$) and Intermediate Porewater Salinities (60–90 G NaCl/L) on the Culturability of Heterotrophic Aerobic Bacteria in Compacted 100% Bentonite.
- Stroes-Gascoyne, S., Hamon, C.J., Maak, P., 2011. Limits to the use of highly compacted bentonite as a deterrent for microbiologically influenced corrosion in a nuclear fuel waste repository. *Phys. Chem. Earth Parts 36*, 1630–1638. <https://doi.org/10.1016/j.pce.2011.07.085>.
- Stroes-Gascoyne, S., Hamon, C.J., Maak, P., Russell, S., 2010. The effects of the physical properties of highly compacted smectitic clay (bentonite) on the culturability of indigenous microorganisms. *Appl. Clay Sci.* 47, 155–162. <https://doi.org/10.1016/j.clay.2008.06.010>.
- Sun, S., Wu, Y., Zhang, J., Wang, G., DeLuca, T.H., Zhu, W., Li, A., Duan, M., He, L., 2019. Soil warming and nitrogen deposition alter soil respiration, microbial community structure and organic carbon composition in a coniferous forest on eastern Tibetan Plateau. *Geoderma* 353, 283–292. <https://doi.org/10.1016/j.geoderma.2019.07.023>.
- Tong, H., Behazin, M., Simpson, M.J., 2023. Assessment of heat and radiation impacts on natural organic matter composition in bentonite for used nuclear fuel disposal. *Appl. Clay Sci.* 232, 106808. <https://doi.org/10.1016/j.clay.2022.106808>.
- Tully, C.S., Binns, W.J., Zagidulin, D., Noël, J.J., 2023. Investigating the effect of bentonite compaction density and environmental conditions on the corrosion of copper materials. *Mater. Corros.* 1, 13. <https://doi.org/10.1002/maco.202313768>.
- Usman, M.O., Simpson, M.J., 2021. Assessment of the molecular-level compositional heterogeneity of natural organic matter in bentonites intended for long-term used nuclear fuel storage. *Org. Geochem.* 152, 104166. <https://doi.org/10.1016/j.orggeochem.2020.104166>.
- Villagran, J., Ben Belfadhel, M., Birch, K., Freire-Canosa, J., Garamszeghy, M., Garisto, F., Gierszewski, P., Gobien, M., Hirschorn, S., Hunt, N., Khan, A., Kremer, E., Kwong, G., Lam, T., Maak, P., McKelvie, J., Medri, C., Murchison, A., Russell, S., Sanchez-Rico Castejon, M., Stahmer, U., Sykes, E., Urrutia-Bustos, A., Vorauer, A., Wanne, T., Yang, T., 2011. RD&D Program 2011 – NWMO's Program for Research, Development and Demonstration for Long-Term Management of Used Nuclear Fuel.
- Volkman, J.K., Revill, A.T., Holdsworth, D.G., Fredericks, D., 2008. Organic matter sources in an enclosed coastal inlet assessed using lipid biomarkers and stable isotopes. *Org. Geochem.* 39, 689–710. <https://doi.org/10.1016/j.orggeochem.2008.02.014>.
- Wilson, J.G., Luczkovich, J.J., 2011. Introduction to food webs in coastal and estuarine ecosystems. In: Wolanski, E., McLusky, D. (Eds.), *Treatise on Estuarine and Coastal Science*. Academic Press, Waltham, pp. 1–4. <https://doi.org/10.1016/B978-0-12-374711-2.00601-X>.
- Zhou, C., Liu, Yunde, Liu, C., Liu, Yuanyuan, T'faily, M.M., 2019. Compositional changes of dissolved organic carbon during its dynamic desorption from hyporheic zone sediments. *Sci. Total Environ.* 658, 16–23. <https://doi.org/10.1016/j.scitotenv.2018.12.189>.